

## Supporting Information

# Interaction of Amphiphilic $\alpha$ -Helical Cell-Penetrating Peptides with Heparan Sulfate

Ji Yang,<sup>a</sup> Hiroshi Tsutsumi,<sup>a</sup> Tadaomi Furuta,<sup>b</sup> Minoru Sakurai,<sup>b</sup> and Hisakazu Mihara<sup>\*a</sup>

<sup>a</sup> Department of Bioengineering, Graduate School of Bioscience and Biotechnology, Tokyo Institute of Technology, Nagatsuta-cho 4259 B-40, Midori-ku, Yokohama 226-8501, Japan

<sup>b</sup> Center for Biological Resources and Informatics, Tokyo Institute of Technology, Nagatsuta-cho 4259-B-62, Midori-ku, Yokohama, 226-8501, Japan

## Materials and Methods

### Materials

All CPPs were synthesized on a TentaGel S RAM Rink-type resin using the standard Fmoc chemistry-based strategy.<sup>1</sup> The crude peptides were purified using RP-HPLC and characterized using ESI-MS. The CPPs used in the fluorescence measurements contained a fluorescent moiety (IAEDANS, 5-({2-[(iodoacetyl)amino]ethyl}amino)naphthalene-1-sulfonic acid) attached to the C-terminal cysteine, and the CPPs used in circular dichroism (CD), dynamic light scattering (DLS), and isothermal titration calorimetry (ITC) analyses contained 2-iodoacetamide (ICH<sub>2</sub>CONH<sub>2</sub>) attached to the C-terminal cysteine to inhibit the formation of disulfide bonds. The fluorophore-conjugated peptide and acetamide-conjugated peptide were prepared as follows. First, IAEDANS or ICH<sub>2</sub>CONH<sub>2</sub> (5  $\mu$ mol) was dissolved in 50% v/v acetonitrile/phosphate buffer (pH 8.0). This solution was added to 1  $\mu$ mol solid-supported CPP and maintained at 37 °C for 1.5 h. The reaction solution of the coupling steps was purified using RP-HPLC and characterized using ESI-MS.

Heparan sulfate (HS) sodium salt (from porcine intestinal mucosa; average molecular weight, 13.6 kDa; sulfur content: 5.43%; nitrogen content: 2.52%) was purchased from Celsus Laboratories. The purified peptides were dissolved in H<sub>2</sub>O at approximately 1 mM and stored at 4 °C. To estimate the concentration of each peptide stock solution, amino acid analysis was performed using a Wakopak WS-PTC column (4.0  $\times$  200 mm; Wako Pure Chemical) on a Shimadzu LC2010C system after hydrolysis in 6 M HCl at 110 °C for 24 h in a sealed tube followed by phenyl isothiocyanate labeling. The solutions used in the experimental assay were prepared with buffer containing 20 mM Tris-HCl and 100 mM NaCl at pH 7.4.

### Circular dichroism spectroscopy

The CD spectra of the peptides were recorded using a JASCO J-720WI spectropolarimeter. The spectra were acquired using a 1-mm path length quartz cuvette at 25 °C from 200 to 250 nm. The spectra of CPP alone were acquired for peptide concentrations varying from 10 to 100  $\mu$ M. A 10  $\mu$ M CPP solution was used to measure the spectra of CPP in the presence of HS at different concentrations. CD data were calculated as the mean residual ellipticity (MRE; deg cm<sup>2</sup> dmol<sup>-1</sup>). The  $\alpha$ -helical content was estimated from the molecular MRE at 222 nm as previously described.<sup>2</sup>

\* Corresponding author. Tel: +81-45-924-5756; Fax: +81-45-924-5833; E-mail: [hmihara@bio.titech.ac.jp](mailto:hmihara@bio.titech.ac.jp).

## Fluorescence spectroscopy

Measurements were performed on a fluorescence microplate reader (Twinkle LB 970) in nonbinding 96-well plates. The excitation and emission filters were set to 340 nm and 460 nm, respectively. The data points were recorded at room temperature 30 times at 15-sec intervals. A fluorescence intensity of the appropriate blank solution was recorded and subtracted from the subsequent fluorescence intensity containing mixtures of CPP and HS. The number of CPP-binding sites in HS for individual CPPs was determined using the Job's method.<sup>3</sup>

A model of a single set of identical sites was used to fit the binding data.<sup>4</sup> Nonlinear least squares analysis of the binding data was generated by employing the following equations to determine the  $K_d$  of the four peptides. Because the initial fluorescence intensity  $F_0$  was not absolutely accurate, a constant  $C_0$  was added to the equation;  $n$  was determined by Job's plot and fixed in the fitting equation.

$$\begin{aligned}\Delta F &= F - F_{CPP} - F_{Background} = (\varepsilon_p[P] + \varepsilon_b[P]_b) - \varepsilon_p[P]_t = (\varepsilon_b - \varepsilon_p)[P]_b = \Delta\varepsilon[P]_b \\ &= \frac{\Delta\varepsilon}{2} \left\{ n[H]_t + [P]_t + K_d - \sqrt{(n[H]_t + [P]_t + K_d)^2 - 4n[H]_t[P]_t} \right\} + C_0\end{aligned}\quad (1)$$

where  $F$ ,  $F_{CPP}$ , and  $F_{Background}$  are the fluorescence intensities of the solutions that contain both CPP and HS, CPP only, and HS only, respectively.  $[P]$  and  $[P]_b$  are the concentrations of free or bound CPP, respectively.  $[P]_t$  and  $[H]_t$  are the total concentrations of CPP or HS, respectively.  $\Delta\varepsilon$  is the difference between the extinction coefficient of free CPP and that of bound CPP.

## Isothermal titration calorimetry

The heat flow resulting from the binding of CPP to HS was measured with highly sensitive isothermal titration calorimetry using a MicroCal VP-ITC calorimeter. Titrations were performed by injecting 25 aliquots of 10  $\mu$ L of HS (8  $\mu$ L of HS for the EF peptide) solution into the CPP solution every 5 min. The CPP concentration in the reaction cell ( $V_{cell} = 1.434$  mL) was 80  $\mu$ M, and the HS concentration in the injection syringe was 200  $\mu$ M. Temperatures were set to 18, 28, 38, or 48  $^{\circ}$ C. Buffer for both solutions was 20 mM Tris-HCl, 100 mM NaCl, pH 7.4. Control titrations were also performed, i.e., the HS solution was injected into pure buffer or pure buffer was injected into CPP solution at different temperatures. All solutions were degassed immediately prior to use. The raw data were processed using the Origin software provided with the instrument. The heats of dilution were subtracted from the heats measured for the binding reaction. For a complete thermodynamic characterization of the binding process, including the association constant  $K_0$ , free energy  $\Delta G^0$ , enthalpy  $\Delta H^0$ , and entropy  $\Delta S^0$ , the calorimetric data were analyzed using an identical multisite binding model, which has also been used to describe the binding equilibrium of other peptides to HS.<sup>5</sup>

## Dynamic light scattering

DLS measurements were performed using a Zetasizer Nano ZEN3690 instrument (Malvern). Measurements were performed in a 1.0 cm-path length acryl cuvette with 400  $\mu$ L of 30  $\mu$ M CPP and different HS concentrations at 25  $^{\circ}$ C. Size information was obtained by analysis of the

autocorrelation function by both CONTIN and second cumulants using the software included with the Zetasizer instrument, and the resulting intensity counts were volume weighted. To estimate the maximum number of HS chains with CPPs in one CPP-HS cluster, the hydrodynamic volume of the cluster was assumed to be spherical ( $V_h = 4/3\pi R_h^3$ ). The structure of the cluster was divided by the volume of a single HS chain saturated with a defined number of CPPs as detected by ITC. The volumes of HS from known protein database entries and  $\alpha$ -helical CPPs were calculated using the software Chem3D (Cambridge) as previously described.<sup>6</sup>

## Molecular dynamics simulations

Each structure (0-4) in **Figure 7** was constructed using the AMBER 12.0 package.<sup>7</sup> The C-terminal cysteine of the CPP was removed from the sequence, which was then capped with NHE (amide ending group). The initial secondary structure of CPP was  $\alpha$ -helix. The HS structure (**Figure S5**) was constructed using 5 major disaccharide patterns of heparin (- (1-4)- $\alpha$ -D-IdoA2S-(1-4)- $\alpha$ -D-GlcNS6S-),<sup>8,9</sup> which were primarily responsible for binding to proteins or peptides. The resultant HS structure is a model of heparin (which is a closely related molecule of HS), but the name HS is used hereafter for consistency. The CPP-HS complex structures were manually constructed by placing the HS near the CPP structure. The ff12SB force field<sup>10</sup> in AMBER 12.0<sup>7</sup> was used for the peptides, and the GLYCAM\_06h-12SB<sup>11</sup> parameter set was used for the HS fragment. The net charge was neutralized by an appropriate number of counter ions (Na<sup>+</sup> or Cl<sup>-</sup>), and the system was solvated using a TIP3P water box.<sup>12</sup>

MD simulations were performed for all of the systems shown in **Figure 7**, and all of the simulations were performed using the AMBER 12.0 package<sup>7</sup> on the supercomputer *Tsubame 2.0*<sup>13</sup>. The simulations consisted of three steps. First, in the minimization step, 100 cycles of the steepest descent algorithm followed by 200 cycles of the conjugate gradient algorithm were performed. Second, in the equilibration step, 0.5-ns simulations of constant temperature equilibration (NVT) followed by 0.5-ns simulations of constant pressure equilibration (NPT) were performed. All of the heavy atoms were restrained with a force constant of 2.0 kcal/(mol Å<sup>2</sup>). In the NVT phase, the system was heated from 0 K to 300.0 K using the weak-coupling algorithm. In the NPT phase, the temperature was maintained at 300.0 K, and the pressure was regulated to 1.0 bar. Third, in the production step, 50-ns simulations with a step time of 2.0 fs (a total of 25,000,000 MD steps) were performed without restraints. The temperature was maintained at 300.0 K, and the pressure was maintained at 1.0 bar. During all of the simulations, bonds involving hydrogen were constrained by SHAKE, the nonbonded cutoff was set to 8.0 Å, and a periodic boundary was used.

The changes in the enthalpy ( $\Delta H$ ) of all of the binding processes (II, III, and IV) shown in **Figure 7** were calculated using the MM/GBSA method during the last 30 ns (from 20 ns to 50 ns) at 10-ps intervals. The changes in the vibrational entropy of the systems,  $T\Delta S$ , were calculated by performing normal mode analyses<sup>14</sup> using the NMODE module. Snapshots at every 750 ps during the last 30-ns simulations were used. The binding free energies ( $\Delta G$ ) were calculated using  $\Delta H - T\Delta S$ . The MD simulation structures were visualized using VMD 1.9.1 (<http://www.ks.uiuc.edu/Research/vmd/>).<sup>15</sup> Other simulation details will be published elsewhere.

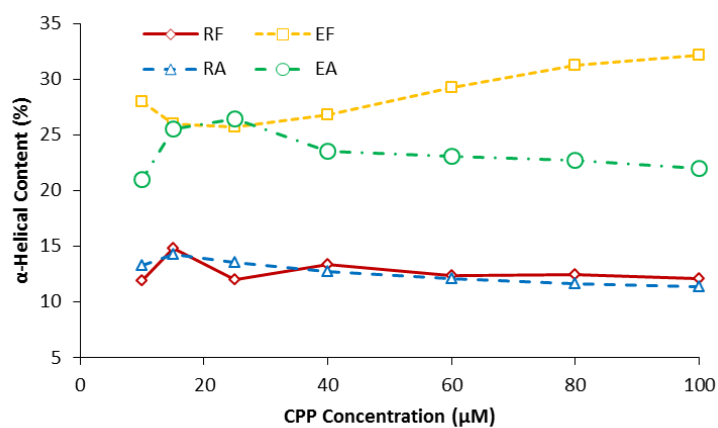
## Supplementary Table

Table S1. CPP activities in different cell lines<sup>16</sup>

Peptide	<u>RF</u>	<u>RA</u>	<u>EF</u>	<u>EA</u>
HeLa	+++	+++	+++	+
A549	+++	++	+++	++
3T3-L1	+	+++	+	+
PC12	—	+++	++	+

## Supplementary Figures

### Circular dichroism



**Figure S1.**  $\alpha$ -Helical contents of the four designed CPPs at different concentration in the absence of HS.

## Fluorescence spectroscopy

A Job's Plot was performed on each CPP to determine the number of CPP-binding sites in HS at a total concentration (CPP + HS) of 10  $\mu\text{M}$  at room temperature. Calculation was based on the following model<sup>3</sup>



where  $P$  is CPP,  $H$  is HS,  $n$  is the number of CPP-binding sites in HS. The expression of the limiting slope of the Job curve ( $[\text{CPP}] \rightarrow 0$  or  $[\text{HS}] \rightarrow 0$ , **Figure S2**) is

$$\left. \frac{d[P_nH]}{df_{HT}} \right|_{f_{HT} \rightarrow 0} = \frac{C_T^{n+1}}{C_T^n + K_d}, \quad \left. \frac{d[P_nH]}{df_{PT}} \right|_{f_{PT} \rightarrow 0} = \frac{C_T^{n+1}}{nC_T^n + K_d} \quad (2)$$

At the intersection point of the two lines, which have the slopes that are described by Eq.(2), we have

$$\frac{f_{PT}}{f_{HT}} = \frac{nC_T^n + K_d}{C_T^n + K_d} \quad (3)$$

where  $f_{PT} = \frac{[P]_T}{[P]_T + [H]_T}$ ,  $f_{HT} = \frac{[H]_T}{[P]_T + [H]_T}$ .  $C_T = [P]_T + [H]_T$  is the total concentration of CPP and HS.

$$\text{if } C_T \gg K_d: \frac{f_{PT}}{f_{HT}} = \frac{f_{PT}}{(1 - f_{PT})} = n \quad (4)$$

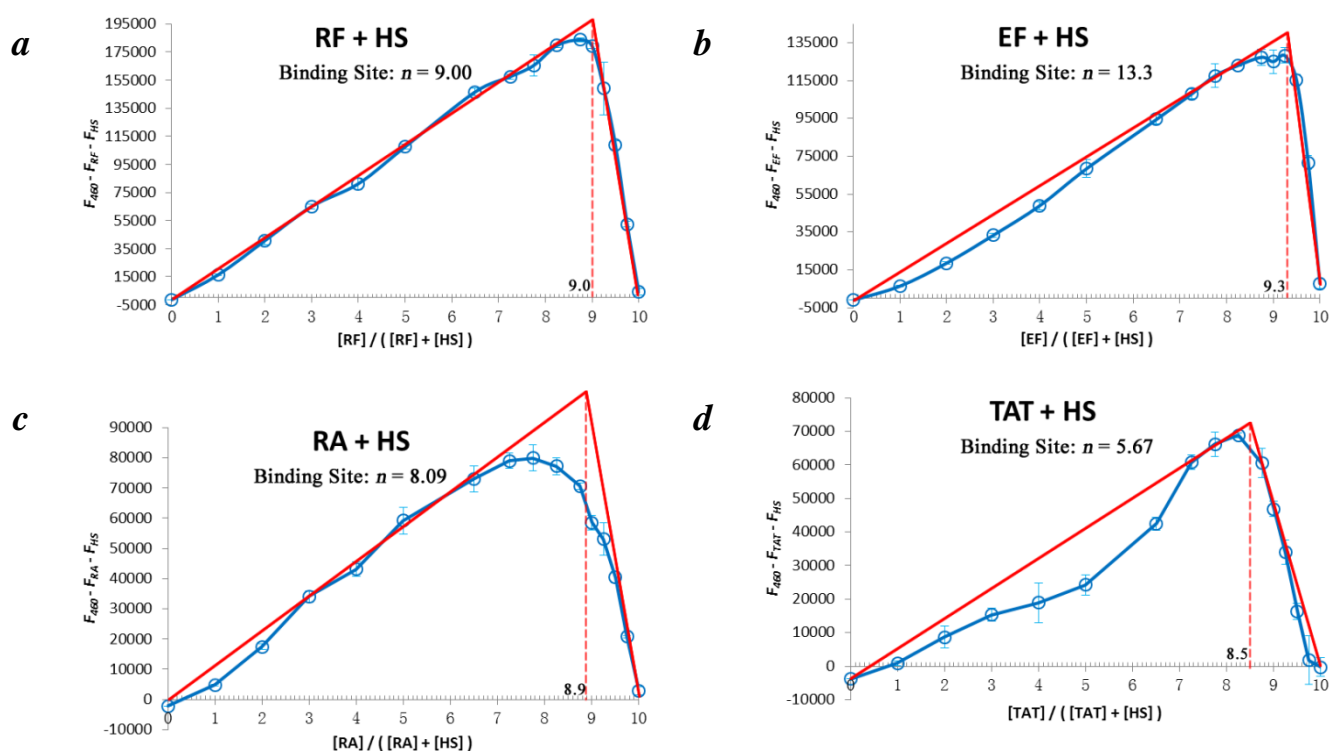


**Figure S2.** Job's Plots of (a) RF, (b) EF, (c) RA, and (d) TAT. The total concentration of CPP and HS is 10  $\mu\text{M}$ .

## Isothermal titration calorimetry

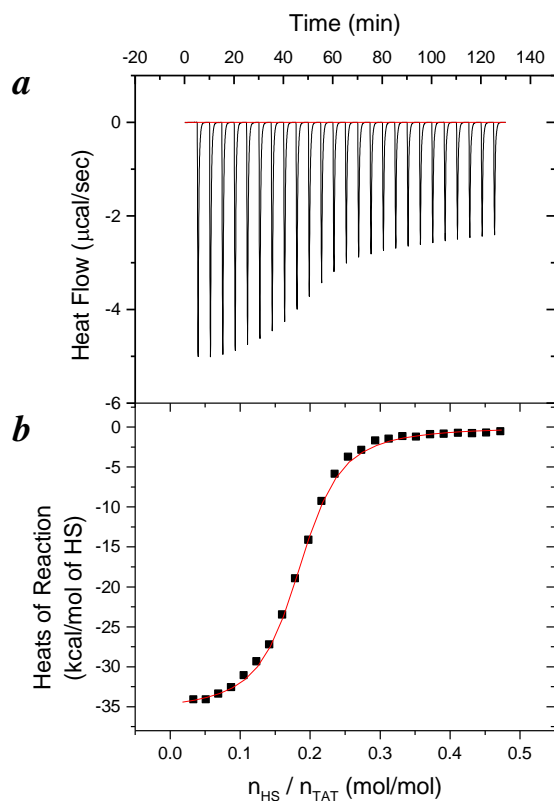


**Figure S3.** Isothermal titration calorimetry. Titration of HS into TAT at 28 °C. (a) Heat flow of titration of HS solution into TAT solution. TAT concentration in the reaction cell ( $V_{\text{cell}} = 1.434 \text{ mL}$ ) was 80  $\mu\text{M}$ , HS concentration in the injection syringe was 200  $\mu\text{M}$ . Buffer for both solutions was 20 mM Tris-HCl, 100 mM NaCl, pH 7.4. (b) Heats of reaction  $h_i$  (integration of the heat flow peaks of (a) and the heats of dilution were subtracted from the heats measured for the binding reaction) as a function of the molar ratio of HS/TAT. Filled squares represent experiment data (■). The solid line is a least-square fit using a model of a single set of identical sites with the parameters listed in **Table 4**.

## Dynamic light scattering

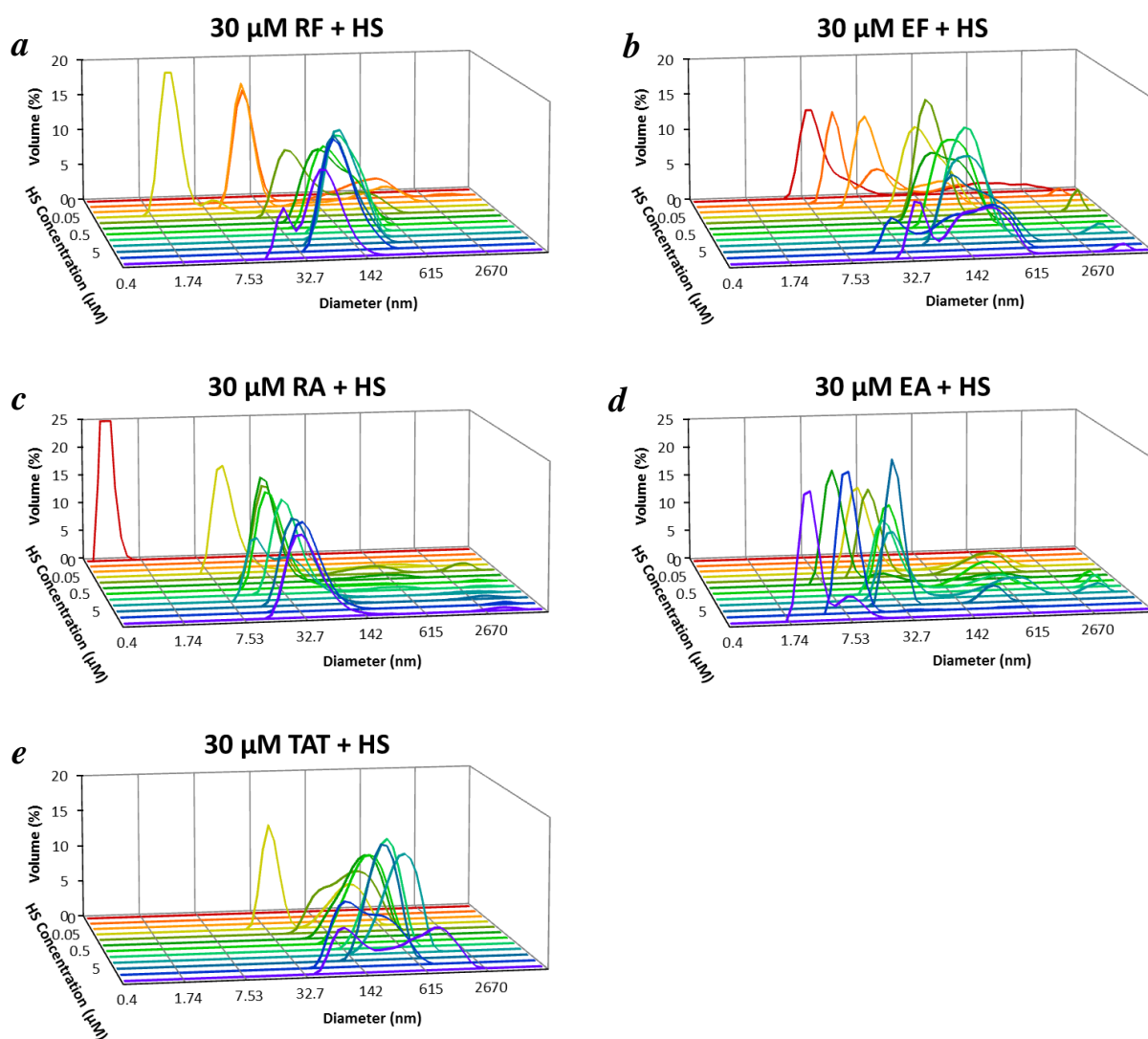


**Figure S4.** Particle size distributions (volume-weighted) of the HS-CPP complexes (*a* RF; *b* EF; *c* RA; *d* EA; *e* TAT). The CPP solution (400  $\mu$ L, 30  $\mu$ M) was titrated with HS in 20 mM Tris-HCl buffer, 100 mM NaCl, pH 7.4, 25  $^{\circ}$ C.

## Molecular dynamics simulations

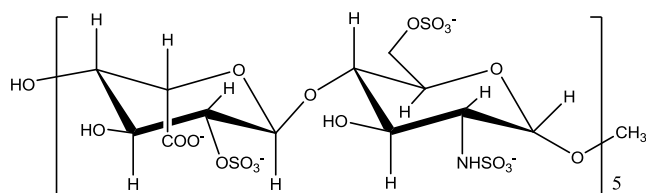


**Figure S5.** Chemical structure of HS used in the simulations. Sulfate esters are emphasized with spheres.

## References

1. K. Usui, K. Y. Tomizaki and H. Mihara, *Bioorg. Med. Chem. Lett.*, 2007, **17**, 167-171.
2. J. M. Scholtz, H. Qian, E. J. York, J. M. Stewart and R. L. Baldwin, *Biopolymers*, 1991, **31**, 1463-1470.
3. C. Y. Huang, *Methods Enzymol.*, 1982, **87**, 509-525.
4. A. Rullo and M. Nitz, *Biopolymers*, 2010, **93**, 290-298.
5. G. Klocek and J. Seelig, *Biochemistry*, 2008, **47**, 2841-2849.
6. A. Ziegler and J. Seelig, *Biophys. J.*, 2008, **94**, 2142-2149.
7. R. Salomon-Ferrer, D. A. Case and R. C. Walker, *Wiley Interdiscip. Rev.: Comput. Mol. Sci.*, 2013, **3**, 198-210.
8. D. L. Rabenstein, *Nat. Prod. Rep.*, 2002, **19**, 312-331.
9. N. S. Gandhi and R. L. Mancera, *Chem. Biol. Drug Des.*, 2008, **72**, 455-482.
10. V. Hornak, R. Abel, A. Okur, B. Strockbine, A. Roitberg and C. Simmerling, *Proteins: Struct., Funct., Bioinf.*, 2006, **65**, 712-725.
11. K. N. Kirschner, A. B. Yongye, S. M. Tschampel, J. Gonzalez-Outeirino, C. R. Daniels, B. L. Foley and R. J. Woods, *J. Comput. Chem.*, 2008, **29**, 622-655.
12. W. L. Jorgensen, J. Chandrasekhar, J. D. Madura, R. W. Impey and M. L. Klein, *J. Chem. Phys.*, 1983, **79**, 926-935.
13. S. Matsuoka, in *High Performance Computing on Vector Systems 2007*, Springer, 2008, pp. 265-267.
14. D. A. Case, *Curr. Opin. Struct. Biol.*, 1994, **4**, 285-290.
15. W. Humphrey, A. Dalke and K. Schulten, *J. Mol. Graph. Model.*, 1996, **14**, 33-38.
16. K. Usui, T. Kikuchi, M. Mie, E. Kobatake and H. Mihara, *Bioorg. Med. Chem.*, 2013, **21**, 2560-2567.